Progress In Electromagnetics Research C, Vol. 113, 13–27, 2021

Design, Optimization, and Analyses of Nano-Optical Couplers Consisting of Nanocubes to Construct Efficient Nanowire Transmission Systems

Aşkın Altınoklu and Özgür Ergül*

Abstract—We present the design, optimization, and analyses of efficient couplers to construct nano-optical transmission systems involving nanowires. The couplers consist of optimized arrangements of nanocubes and are integrated into critical locations, such as nanowire inputs, corners, and junctions, to improve electromagnetic transmission in accordance with design purposes. Optimization and numerical analyses are performed by employing an efficient simulation environment based on a full-wave solver and genetic algorithms. Using the designed couplers, we obtain various configurations that enable efficient transmission and distribution of input powers to multiple outputs. With their favorable properties, the designed couplers and constructed systems can be further used to build larger nanowire networks.

1. INTRODUCTION

Using the plasmonic properties of metals at optical frequencies, nanowires are excellent tools to efficiently transmit electromagnetic power across long distances with respect to wavelength [1–13]. However, as in all transmission systems, their capabilities can be dramatically deteriorated due to physical deformations and defects. For example, significant power losses are observed even for smoothly bent nanowires [8], when these structures deviate from their ideally straight shapes, indicating that even changing the direction of the power flow in a nanowire system is a fundamental issue. In such applications involving the redirection of transmission, supporting nanowires with other nano-optical components can provide remarkable results. In our recent efforts [13], we have developed this kind of compact couplers involving optimal arrangements of nanoparticles, usually nanocubes. As shown via computational simulations, these well-designed couplers can significantly improve transmission along bent nanowires, even with sharp corners. The effectiveness of the developed corner couplers has motivated us to use the proposed approach to build similar couplers that may enable the construction of more complex nanowire systems with multiple segments.

In this study, we consider nanowire transmission systems involving alternative combinations of nanowires. In each system, the purpose is to efficiently transmit electromagnetic power from the input to output or to multiple outputs. Without using any supporting mechanism, simple connections of nanowires do not provide the desired characteristics due to sharp corners and junctions, where reflections and diffractions prevent efficient transmissions. We design various couplers that can be easily used in alternative junction types, as well as for the efficient coupling between excitations and nanowires. Each coupler is an optimal arrangement of nanocubes, which also possess plasmonic properties, integrated into a critical position to enhance the function of the corresponding system. The optimal configuration for a given set of nanocubes is found by considering the entire combination of nanowires and the coupler as a full-wave optimization problem and analyzing candidate solutions via the multilevel fast multipole

Received 14 March 2021, Accepted 17 May 2021, Scheduled 18 May 2021
* Corresponding author: Özgür Ergül (ozergul@metu.edu.tr).
The authors are with the Department of Electrical and Electronics Engineering, Middle East Technical University, Ankara, Turkey.

algorithm (MLFMA) [14, 15]. Among alternative choices, genetic algorithms (GAs) are preferred to heuristically but effectively reach optimal coupler designs. Each optimization problem requires thousands of simulations, which can be handled thanks to the efficiency of the MLFMA implementation developed particularly for plasmonic problems [16]. Integration of GAs and MLFMA into a single optimization environment via a dynamic accuracy control [17] further facilitates accurate and efficient designs of couplers. Our preliminary results on the design of corner and input couplers, in addition to attempts to integrate multiple couplers, can be found in [13, 18, 19].

Finding an optimal configuration of nanocubes with required electromagnetic characteristics is not sufficient for the design of a nano-optical coupler. In addition to nanowire transmission systems as final products, this paper presents the overall process by exemplifying fine-tuning operations and sensitivity analyses, as well as the generation of importance maps and frequency responses. Using a subsystem approach, the couplers are designed independently so that their integration into a single system needs initial tests with alternative combinations. At the end, using the designed couplers and nanowire segments, we present five different transmission systems that efficiently divide the input power into two, three, four, and five outputs, respectively. Power density values obtained at the outputs demonstrate the excellent transmission characteristics of the systems, as well as the possibility to use them to construct even larger systems towards nano-optical networks.

2. NANO-OPTICAL COUPLERS CONSISTING OF NANOCUBES

2.1. Simulation and Optimization Environment

For the simulation and optimization of the systems involving nanowires and couplers, MLFMA and GAs are integrated into a single environment. This is particularly performed to facilitate dynamic accuracy control [17], i.e., a strategy based on the adjustment of the MLFMA accuracy in the course of the optimization. While designing couplers via GAs, each individual (candidate design) is considered as a three-dimensional electromagnetic problem to be solved via MLFMA. Hence, in a typical optimization involving thousands of trials, thousands of MLFMA simulations are required. Using initial-guess between consecutive solutions does not provide a significant acceleration, since even a single nanocube may dramatically change the characteristics of the overall structure. Therefore, advanced strategies like dynamic accuracy control are needed for efficient optimization attempts. In this strategy, candidate designs during an optimization are not solved with the same level of accuracy. In addition to the standard MLFMA, approximate (and faster) versions are used, whose inaccuracy levels are reflected to the fitness values of the individuals. Specifically, when an individual is analyzed by using an approximate MLFMA, the obtained fitness value is reduced by the predicted inaccuracy margin (uncertainty) of the approximation. This way, the evaluation of the initial generations is greatly accelerated, while the accuracy levels of MLFMA versions are automatically updated towards the end of an optimization with the increased confidence on the successful individuals. The final generations are carried out via full MLFMA simulations, which can provide accurate results with maximum 1% error in current coefficients.

Plasmonic properties of the analyzed structures lead to numerically challenging simulations in terms of efficiency and accuracy. In the context of surface formulations, we prefer the modified combined tangential formulation (MCTF) [20] for accurate solutions of plasmonic structures. MCTF is particularly essential for the problems considered in this paper, where nanowires and nanocubes are made of Ag and analyzed at 250 THz. At this frequency, Ag has a relative permittivity of approximately $-61 + 4.3i$, with a large negative real part that causes numerical issues in the conventional formulations. Although MCTF is accurate in modeling objects with such permittivity values, it is a first-kind integral-equation formulation that needs extra efforts in iterative solutions. For this purpose, we employ a multilayer iterative strategy, where MLFMA and its approximate versions are used in an inner-outer scheme [21]. The approximate versions of MLFMA both within iterative solutions (in the multilayer strategy) and in the course of an optimization (for the dynamic accuracy control) are obtained by a systemic reduction of harmonics (plane waves) used to compute far-zone interactions. MCTF is discretized by using the conventional Rao-Wilton-Glisson functions [22] to expand the electric and magnetic currents on triangulated surfaces. For a typical nanowire system considered in this paper, the number of unknowns is limited to 50,000, while large electrical sizes lead to many levels in tree structures of MLFMA.

The MLFMA implementation used for the simulations is based on the standard diagonalization of the Green's function via plane waves [14]. For a given object, we first construct the multilevel tree structure by placing the object in a computational box and recursively dividing it into smaller boxes. The smallest box size is set to $\lambda/4$, where $\lambda \approx 1.2\,\mu\text{m}$ is the wavelength in the host medium (vacuum) for the problems considered in this study. Near-zone and far-zone interactions are organized according to a one-box-buffer scheme. Given a vector of N current coefficients $\mathbf{x}$ during an iterative solution, for either the electric current density or the magnetic current density, MLFMA performs a matrix-vector multiplication as

$$\mathbf{y} = \bar{\mathbf{Z}}^{\text{NF}} \cdot \mathbf{x} + \bar{\mathbf{Z}}^{\text{FF}} \cdot \mathbf{x}, \tag{1}$$

where $\bar{\mathbf{Z}}^{\text{NF}}$ and $\bar{\mathbf{Z}}^{\text{FF}}$ represent the near-zone and far-zone interactions, respectively, of the considered matrix block. The multiplication related to the far-zone interactions is performed on-the-fly, via aggregation-translation-disaggregation cycles. At the lowest level, an aggregation step starts by adding radiation patterns of basis functions ($\mathbf{S}_n$ for $n = 1, \ldots, N$) at box centers ($\mathbf{r}_C$) as

$$\mathbf{S}_C(\mathbf{r}_C) = \sum_{n \in C} \mathbf{x}[n] \mathbf{S}_n(\mathbf{r}_C), \tag{2}$$

where $\mathbf{S}_n(\mathbf{r}_C)$ depends on the integro-differential operator. Then, from the lowest level to the highest level, radiated fields are obtained as

$$\mathbf{S}_C(\mathbf{r}_C) = \sum_{C' \in C} \beta(\mathbf{r}_C - \mathbf{r}_{C'}) \mathbf{S}_{C'}(\mathbf{r}_{C'}), \tag{3}$$

where β refers to diagonal shift functions. From a level to the higher level, these shifting operations are accompanied by up-sampling via Lagrange interpolation. Once the aggregation step is completed, translations are performed within levels to obtain incoming waves as

$$\mathbf{G}_C\left(\mathbf{r}_C\right) = \sum_{C' \in F\{C\}} \alpha\left(\mathbf{r}_C - \mathbf{r}_{C'}\right) \mathbf{S}_{C'}\left(\mathbf{r}_{C'}\right), \tag{4}$$

where $F\{C\}$ represents far-zone boxes for a given box C, and α refers to diagonal translation functions. In the disaggregation step, the total incoming fields are obtained from the highest level to the lowest level as

$$\mathbf{G}_C^{+}\left(\mathbf{r}_C\right) = \mathbf{G}_C\left(\mathbf{r}_C\right) + \beta\left(\mathbf{r}_C - \mathbf{r}_{C'}\right) \mathbf{G}_{C'}^{+}\left(\mathbf{r}_{C'}\right) \qquad \left(C \in C'\right), \tag{5}$$

where Lagrange anterpolation is used for down-sampling. Finally, the matrix-vector multiplication is completed via an integral over all directions (plane waves) as

$$\left\{\bar{\mathbf{Z}}^{\text{FF}} \cdot \mathbf{x}\right\}[m] \propto \int d^2\hat{\mathbf{k}} \mathbf{F}_m(\mathbf{r}_C) \cdot \mathbf{G}_C^{+}(\mathbf{r}_C) \tag{6}$$

for $m = 1, \ldots, N$, where receiving patterns of testing functions ($\mathbf{F}_m$) are employed.

We emphasize that the aggregation-translation-disaggregation cycle briefly described above must be performed separately for the inner (plasmonic) and outer (vacuum) media. Since some of the inner-medium interactions (in an inner problem based on the equivalence principle) tend to decay rapidly, we further use an interaction-elimination strategy [16] to avoid unnecessary computations that do not have any effect on the accuracy. Further descriptions on the components of MLFMA can be found in [15].

2.2. General Properties of Nanowires and Couplers

The results presented in this paper illustrate the general approach to build nanowire transmission systems involving optimal couplers at critical locations. At the same time, we need to fix some of the geometric properties in order to demonstrate operation principles and properties of these structures via examples. First, the structures involve pairs of Ag nanowires to transmit electromagnetic power from an input to an output or outputs. Each nanowire has a $100 \times 100\,\text{nm}$ square cross section, and the surface-to-surface distance between two nanowires (of a pair) is also fixed to 100 nm. All nanowire systems are assumed to be located in vacuum. For an excitation of a nanowire system, a pair of Hertzian dipoles is used. These dipoles are oriented in opposite directions and located 200 nm away from the nanowire tips.

Also being located in vacuum, power radiated by a Hertzian pair is not efficiently coupled to nanowires, which necessitates a design of an input coupler, as included in the results. While the frequency is fixed to 250 THz in all designs and simulations, the structures are generally able to operate in wide frequency bands (see Section 2.8). We also emphasize that, in the considered frequency range, weak surface plasmon polaritons lead to strong electromagnetic interactions between the components (nanowires and coupler elements) that need full-wave simulations for accurate analyses.

In the nano-optical systems considered in this paper, the nanowires do not possess any discontinuity. For a given connected structure of nanowires with corners and junctions, the designed couplers are integrated into critical locations without any direct physical contact, in order to improve the power transmission from the input to the output(s). In general, the aim is to improve coupling at the input and transmission through sharp corners, while junction couplers are designed to balance power distributions among outputs in addition to maintaining efficient transmissions. To evaluate power transmission performances, we define sample frames near the output tips of the nanowires. For example, in the results of this paper, 1.3×1.3 μm square frames at 100 nm distances from the tips are employed. Then, for a given output, the average of the power density is used to assess the quality of transmission.

Based on our previous experience with various nanoparticles [13], the couplers in this study consist of Ag nanocubes. Specifically, two-dimensional arrays of nanocubes are considered to build optimal couplers in accordance with the design purposes. To be consistent with the nanowires, the dimensions are selected as $90 \times 90 \times 90$ nm, leaving 10 nm surface-to-surface distances between the nanocubes. For each coupler type, a predetermined full grid is defined by only omitting nanocubes that coincide with nanowire locations. Then, by performing an on-off optimization via GAs, the optimal coupler, i.e., an irregular grid of remaining nanocubes, is found.

2.3. Optimization Process

As discussed in Section 2.4, the couplers are designed independently; for a given scenario involving nanowires and a critical location, a single coupler is designed without considering the remaining parts of the overall system. Despite the lack of interaction between subsystems, this approach enables easier optimization and analyses of each coupler, while the results demonstrate that the designed couplers operate in harmony when they are integrated into the same system. In addition, a designed subsystem can be used in diverse configurations in multiple system designs rather than being a part of a fixed system that limit the applicability of the couplers. In fact, attempts to design multiple couplers simultaneously often lead to worse results (in comparison to individual optimization processes) due to the enlarged optimization spaces to be handled by GAs. The success of individual design procedures may partially be due to the relatively long nanowire segments (5 μm) that separate critical regions, while alternative strategies may be needed for nearby couplers.

In an on-off optimization, each nanocube of the given grid is represented by a bit (0/1); the nanocube either exists or not, independent of other nanocubes. For a grid involving only 100 nanocubes, this leads to $2^{100} \approx 1.27 \times 10^{30}$ different configurations that form the optimization space. For some coupler designs, symmetry is enforced to effectively reduce the optimization space. Using pools of 40 individuals, GA operations are performed in general for 200 generations, leading to a total of maximum 8000 MLFMA simulations. By employing a dynamic accuracy control described in Section 2.1, not all MLFMA simulations are performed with full accuracy, while the final results (individuals in the last generations) are guaranteed to be obtained with maximum 1% error. We note that the fitness of an individual is found by an MLFMA solution followed by a post-processing involving the computation of power density values in the output frames. Once the configuration that provides the best fitness value is obtained, the corresponding coupler and the overall geometry are further analyzed. As the current coefficients are already available for the best configuration, these analyses involve the computation of near-zone electric and magnetic fields, as well as power density distributions at various locations around the structure.

2.4. Coupler Types

Figure 1 presents five different types of couplers considered in this paper. For each coupler design, a specific scenario is used in the optimization process, depending on the purpose. On the other hand, the

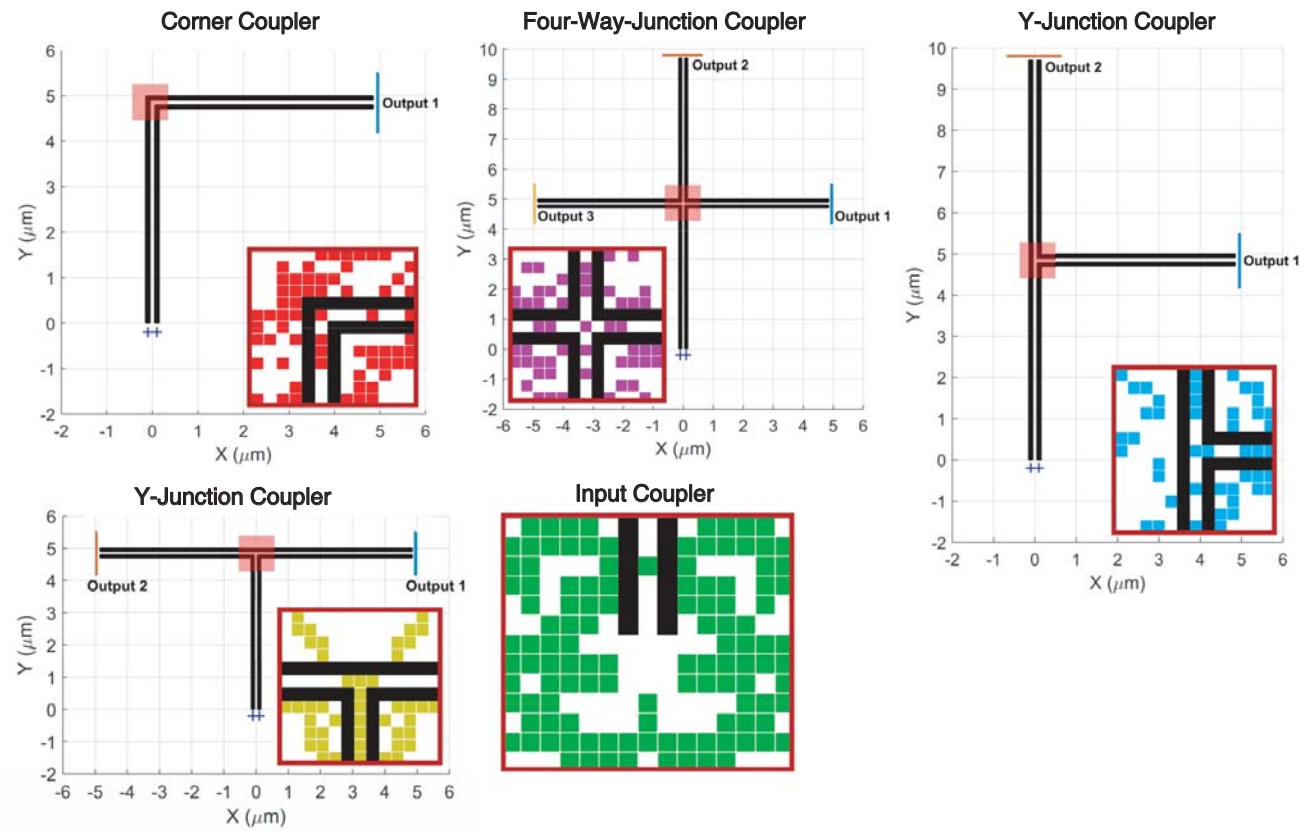

Figure 1. Five different coupler designs and the optimization configurations used to design them: Corner coupler (CC), four-way-junction coupler (FC), Y-junction coupler (YC), T-junction coupler (TC), and input coupler (IC). For the FC, YC, and TC, the fitness value is defined as the average of the mean power density at the outputs.

operation performance of a designed coupler is not strictly limited to the design scenario. For example, the corner coupler (CC) involving 61 nanocubes in Fig. 1 is designed to maximize the mean power density in the output frame when it is used at a sharp corner on a $5 + 5\,\mu$m nanowire pair. At the same time, the CC operates as desired with a reasonable performance for nanowires of various lengths, as well as when these nanowires are connected to others directly or via couplers. The four-way-junction coupler (FC) involving 51 nanocubes is designed to increase the mean power density at three outputs, while minimizing the variation between them. As shown in Fig. 1, the coupler is optimized when it is located at the junction of four $5\,\mu$m nanowire pairs with direct connections between perpendicular segments. In the case of the Y-junction coupler (YC), the purpose is to equally transmit electromagnetic power toward forward and perpendicular directions, while the nanowire segments again have $5\,\mu$m lengths. The T-junction coupler (TC) is used for a similar purpose but in a symmetric case. Finally, the input coupler (IC) is designed to couple an excitation (a pair of Hertzian dipoles) to a pair of nanowires, and it is optimized to maximize the mean power density at the output when the nanowires are straight with $5\,\mu$m lengths.

2.5. Fine-Tuning

As discussed in Section 2.3, the couplers are designed via on-off optimization processes; starting with a full grid, nanocubes are extracted or kept to reach desired transmission characteristics. On the other hand, once an on-off optimization process is completed, it is possible to apply a fine-tuning by performing various geometric modifications to further improve the design. Such a fine-tuning operation can be a part of the overall optimization process, as depicted in Fig. 2 for the IC. Once the optimal

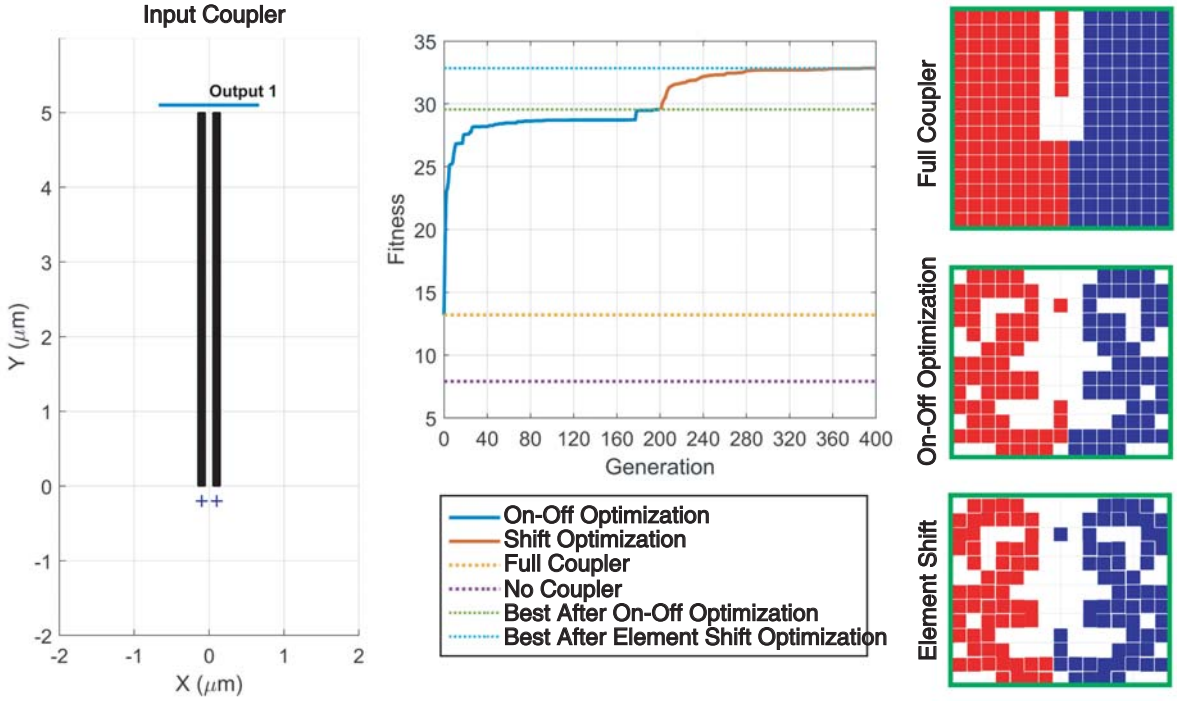

Figure 2. Design of the IC. The fitness value (the best in the pool) is shown with respect to GA generations. Improvement by a fine-tuning operation involving nanocube shifts is also shown. The coupler is designed as a symmetric structure.

on-off configuration is found within 200 GA generations, the kept nanocubes are shifted in the plane of the coupler without allowing them touch each other. As one can observe in the fitness graph, these shifts further improve the performance of the coupler, while such an improvement is typically limited in comparison to the development in the main (on-off) optimization. The same graph includes the fitness values for the full-coupler (the starting point) and no-coupler cases, in order to illustrate the success of the optimization.

2.6. Importance Maps

After a coupler is designed, it is desirable to understand the importance of the kept nanocubes, as well as the extracted ones on the performance of the coupler. Since it is not feasible to test all possible configurations (otherwise optimization would not be necessary), we generate importance maps that reveal the importance of each individual nanocube, either kept or extracted. This type of a map is particularly useful to identify critical locations that must be occupied by nanocubes or those better to remain empty. Fig. 3 presents the importance map for three of the five couplers, namely, the YC, TC, and IC. In each map, the full grid of the coupler is illustrated, where nanocubes are colored based on their effects on the fitness value. For example, a value of 0.5 indicates that an extraction of a nanocube (if it was kept as the result of the optimization) or the insertion of a nanocube (if it was extracted as the result of the optimization), without any change on the other nanocubes, leads to 50% reduction in the fitness value. Hence, in the importance maps, most values are concentrated just below 1.0 (small degradation on the performances of the couplers), while some nanocubes seem to play extremely critical roles. It is remarkable that, for the YJ and TJ, the most critical nanocubes are located at the corners, and they must be absent to achieve the desired operation performances. For the IC, the two critical nanocubes are located at the two symmetric locations near the nanowires. These nanocubes must be kept for a proper operation of the coupler, and the absence of only one of them reduces the fitness (mean power density at the output) five-fold. We note that it is possible to get improvement by switching the

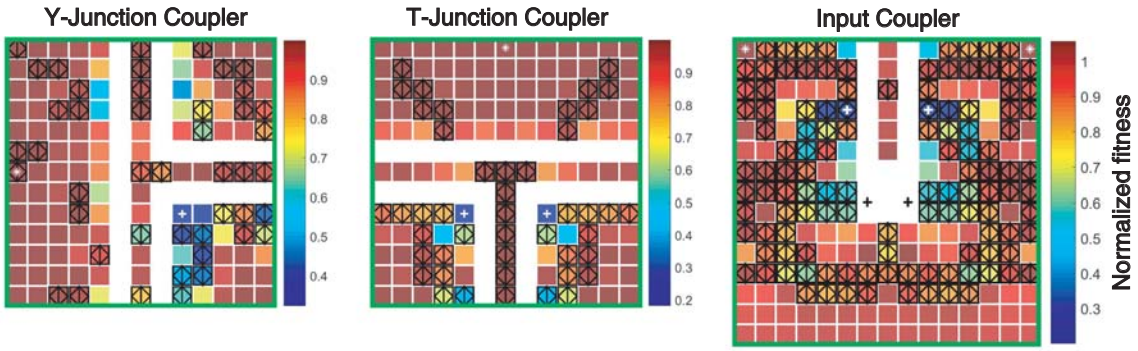

Figure 3. Importance maps for the YC, TC, and IC. The most critical nanocubes (exist or not) are labeled with the + sign.

status of a nanocube (a value greater than 1.0 in Fig. 3), while this occurs rarely (only a few cases in the IC) and leads to a very limited enhancement on the top of the optimization.

2.7. Sensitivity Analyses

Another concern regarding the designed couplers is their sensitivity to various errors that may occur during their fabrication. Therefore, each design is exposed to various operations to test its sensitivity to such deformations. One example is presented in Fig. 4, where the IC is investigated in detail. Two different deformations are considered: (i) random shifts of the nanocubes to test positional errors;

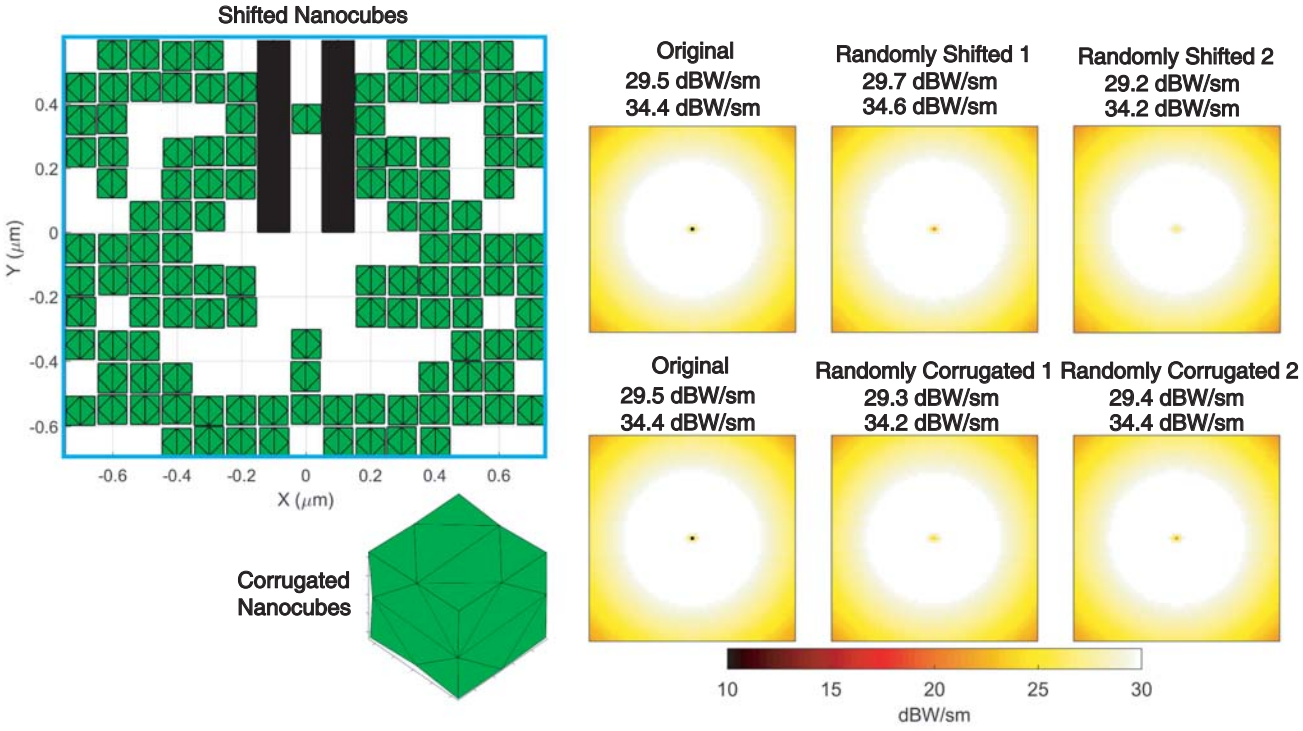

Figure 4. Examples to sensitivity analyses applied on the IC: nanocubes are randomly shifted and nanocube surfaces are randomly corrugated. Results obtained for four different deformed models are compared to the original one obtained for the perfect model. In the plots, the power density distributions in the output frame are shown.

(ii) random corrugations of nanocube surfaces to test element deformations. In a shifting test, each nanocube is independently allowed to be shifted in the $[-3, 3]$ nm range in the x, y, and z directions. In these modifications, the nanocubes keep their perfect cubic shapes. In a surface deformation test, however, each discretization node is independently allowed to move in the $[-2, 2]$ nm range (again in the x, y, and z directions) so that each nanocube has a unique deformed (corrugated) shape in the modified model of the coupler. In all cases, uniform distribution is used to determine random values within the given ranges. Fig 4 presents the results for four different tests: The power density distributions at the output of the 5 μm nanowires are shown for two models with shifted nanocubes and two models with corrugated nanocubes, in comparison to the distribution obtained with the perfect model. We observe that the distributions are almost identical and the effects of random deformations can be understood by inspecting power density values. For the perfect model, the mean/maximum power density values are 29.5/34.4 dBW/sm, while they become 29.7/34.6 dBW/sm and 29.2/34.2 dBW/sm in the shifting tests. In the corrugation tests, these values are 29.3/34.2 dBW/sm and 29.4/34.4 dBW/sm. Hence, geometric deformations have little effects on the performance of the coupler, while they may even provide slight improvements in some cases.

2.8. Frequency Response

As mentioned in Section 2.2, all systems involving nanowires and couplers are designed to operate at 250 THz. At the same time, they maintain good performances at both lower and higher frequencies around 250 THz. One example is depicted in Fig. 5, where the performance of the IC is considered at different frequencies from 200 THz and 300 THz. Without using the IC, the nanowire pair provides moderate levels of transmission, leading to a range of mean power density values at the output from 6 dBW/sm to 12 dBW/sm. The oscillatory nature of the transmission with respect to the frequency is also remarkable. Using the IC designed at 250 THz, the best performance is achieved in the 250–260 THz range with nearly 30 dBW/sm mean power density values at the output. In addition, the values are larger than 20 dBW/sm in a 70 THz range, while they are always well above those obtained for the no-coupler case. Although it is shown only of the IC, all designed couplers have favorable properties in terms of the frequency bandwidth; but, it is also evident in Fig. 5 that an optimization needs to be repeated to re-design a high-performance coupler in case of dramatic changes in the frequency.

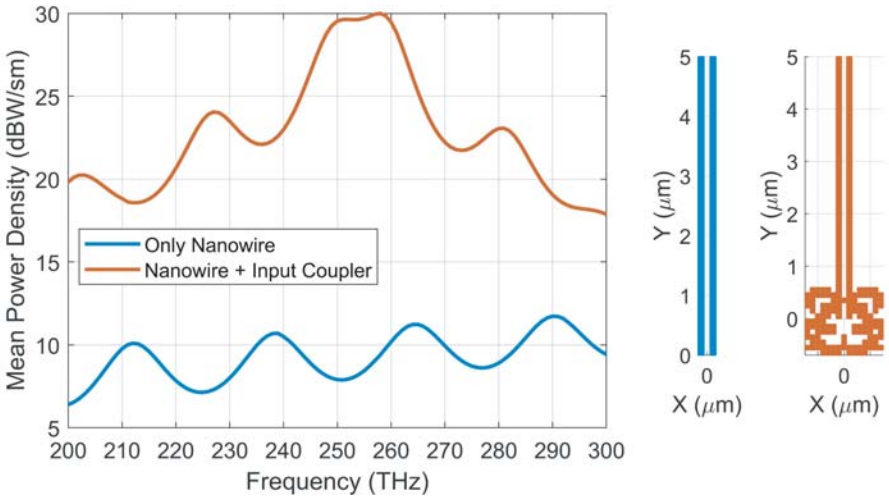

Figure 5. Frequency response of the IC. The mean power density at the output of the nanowire pair is plotted with respect to frequency, both without any coupler and with the IC.

3. COMBINATIONS OF COUPLERS

Although the couplers are designed separately, each in a specific scenario, they maintain high-quality operations when combined and used together to construct nanowire systems. Before designing and building larger systems, however, various initial combinations are considered and tested via comparisons. One of the most basic set of scenarios is depicted in Fig. 6, where a combination of the IC with the CC are studied. On the left panel, the operation of the IC is demonstrated on a 5 µm nanowire pair. As this is the exact scenario for the optimization of the IC, it significantly improves the power transmission leading to 29.5/34.4 dBW/sm mean/maximum power density at the output (in comparison to 7.9/12.8 dBW/sm without the IC). On the right panel of Fig. 6, we consider a $5 + 5$ µm nanowire pair with a sharp corner, which corresponds to the scenario for the optimization of the CC. Using the CC, the mean/maximum power density values at the output are increased from −3.1/8.2 dBW/sm to 7.2/12.0 dBW/sm. As a remarkable observation, using the IC at the input of the pair (without using the CC) leads to 16.4/27.7 dBW/sm, even though the IC is not designed for this scenario. Most importantly, using the IC and CC together provides the best results with 24.4/29.1 dBW/sm mean/maximum power density values. In this overall system, the IC enables the efficient coupling of the power to the nanowires, while the CC enables efficient transmission through the corner by minimizing electromagnetic waves escaping to vacuum. Hence, the couplers operate in harmony to provide the best transmission along the nanowires from the input to the output.

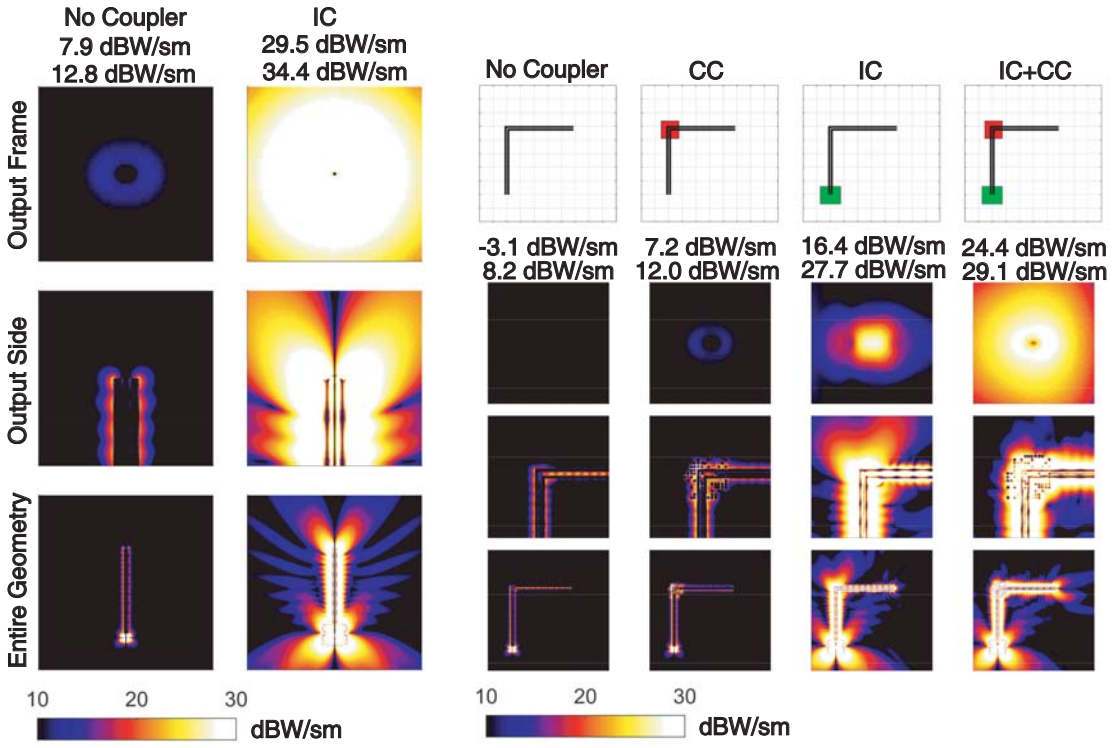

Figure 6. Combination of the IC with the CC on a $5 + 5$ µm nanowire pair with a sharp corner. The best transmission is achieved when the couplers are used together.

Another set of results involving a combination of the IC with the FC is illustrated in Fig. 7. In these results, we consider a four-way junction at the intersection of 5 µm nanowire segments, i.e., the scenario used for the optimization of the FC. Using one of the segments as the input line, the outputs are defined at the end of the other three segments. Without using any coupler, the maximum power density is obtained as 6.4 dBW/sm at two of the outputs (Output 1 and Output 3), while it is only 2.1 dBW/sm at Output 2. Simply filling the junction region with a full grid of nanocubes makes the transmission even worse. Using the FC, however, we achieve 7.5 dBW/sm, 7.2 dBW/sm, and 7.4 dBW/sm maximum

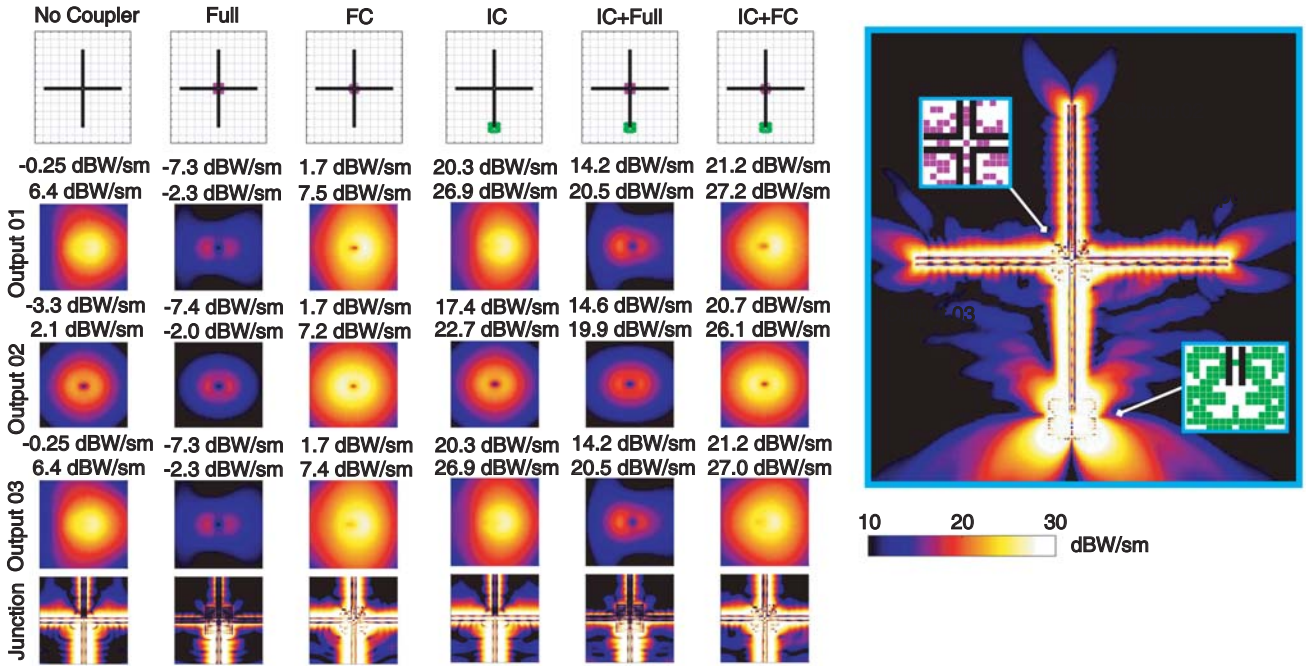

Figure 7. Combination of the IC with the FC on a system involving 5 μm nanowire segments and a four-way junction. The best transmission is achieved when the couplers are used together.

power density values at Output 1, Output 2, and Output 3, respectively. Similar to the previous results in Fig. 6, using the IC alone leads to significantly improved transmissions. Specifically, even without the FC, we obtain 22.7–26.9 dBW/sm maximum power density values. Using a full grid at the junction in addition to the IC blocks the transmission and reduces the output values. We again obtain the best results when both IC and FC are used together. Note that the purpose of the FC is not only improving the transmission to the outputs but also equally distributing the power among them. In the full system involving the IC and FC, the mean power density values are successfully obtained as 21.2 dBW/sm, 20.7 dBW/sm, and 21.1 dBW/sm, with only 0.5 dB margin between Output 1 and Output 2.

Figure 8 presents further experiments involving the combinations of the IC, FC, and TC. On the left panel, we consider the Y-junction involving three 5 μm nanowire segments. Although using the IC alone provides very good transmission properties, the outputs are not well balanced with 19.0/25.8 dBW/sm and 24.2/30.5 dBW/sm mean/maximum power density values. Using the YC in addition to the IC, the transmission ability of the structure is maintained, while the power density values become 22.5/28.2 dBW/sm and 22.5/27.9 dBW/sm (again given as mean/maximum) with an excellent balance in terms of the mean power density. On the right panel, the combination of the IC with the TC is considered on the T-junction scenario. Due to the perfect symmetry, only one of the outputs is considered, in addition to the junction region and the entire geometry, as usual. Using the TC increases the maximum power density from 6.0 dBW/sm to 9.6 dBW/sm at the outputs, while the IC alone leads to 26.2 dBW/sm. We obtain the best result when the two couplers are used together, leading to 22.7/28.3 dBW/sm mean/maximum power density values at the outputs.

4. NANOWIRE SYSTEMS

Finally, we present examples to nanowire transmission systems involving multiple (three or more) couplers. We particularly consider designs with increasing numbers of outputs to demonstrate the effectiveness of the couplers, as well as to exemplify the variety of combinations that they offer to build alternative systems with different functions.

First, Fig. 9 depicts the results for a balanced power splitter, which involves an input segment, a T-junction that connects the input segment to two opposite horizontal segments, and two corners

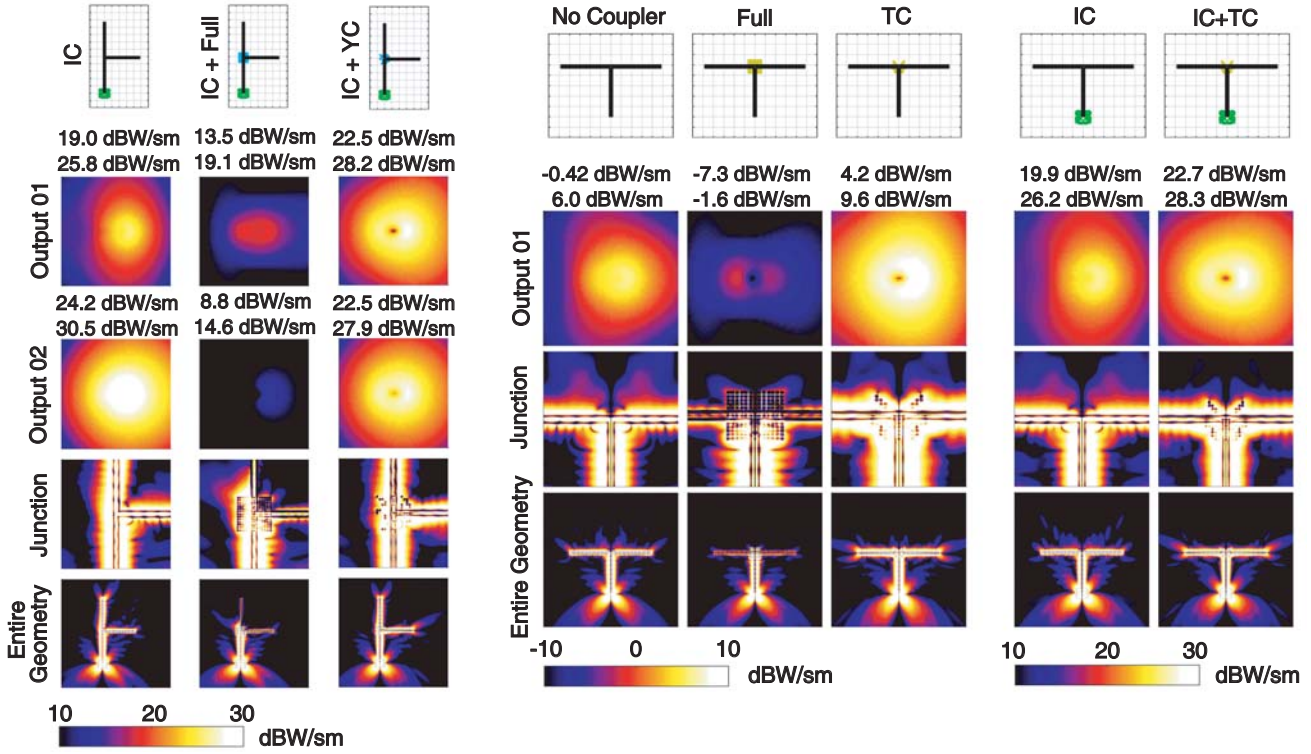

Figure 8. Combination of the YC or TC with the IC in three-way junction scenarios. In both cases, the best transmission results are obtained when the couplers are used together.

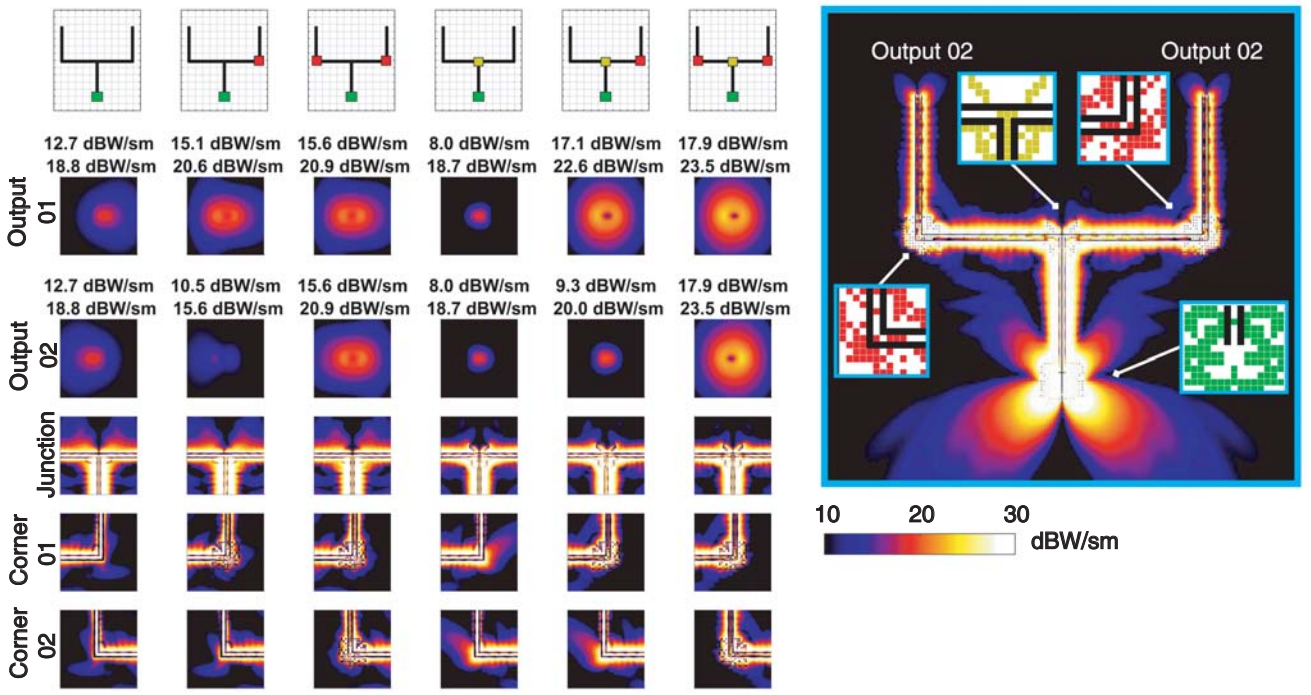

Figure 9. A power splitter involving five nanowire segments, each with 5 µm length. The full system with an efficient transmission involves one IC, one TC, and two CCs at suitable locations.

between the horizontal and vertical (output) segments. Each segment has a 5 μm length so that the entire geometry covers an approximately 10×10 μm area. As expected, the power transmission towards the outputs can significantly be improved by using one IC (at the input), one TC (at the junction), and two CCs (at the corners). Fig. 9 presents not only this configuration, but also incomplete cases involving one, two, or three missing couplers. In all cases, power distributions in the output frames, as well as at the junction and corner regions, are shown. In addition, the entire view of the power distribution for the complete structure with all couplers is illustrated separately. We observe that the mean/maximum power density values at the outputs are increased from 12.7/18.8 dBW/sm to 17.9/23.5 dBW/sm when the TC and CCs are used besides the IC. It is remarkable that using CCs (without the TC) partially improves the transmission (15.6/20.9 dBW/sm), while using the TC deteriorates the results (8.0/18.7 dBW/sm) if it is not accompanied by CCs.

Figure 10 presents another system, which involves a total of five 5 μm nanowire segments to create three outputs. For this system, using the IC significantly improves the power transmission to all three outputs with 18.2 dBW/sm, 15.8 dBW/sm, and 20.1 dBW/sm mean power density values, respectively. If the first Y-junction is supported by the YC, the incoming power is distributed between Output 1 (22.2 dBW/sm mean power density) and the other two outputs (14.4 dBW/sm and 16.9 dBW/sm mean power density values). On the other hand, using two YCs (at both junctions), we reach a more balanced distribution between Output 2 and Output 3 (16.9 dBW/sm and 16.0 dBW/sm mean power density values), in addition to an efficient transmission to Output 1 (22.4 dBW/sm mean power density).

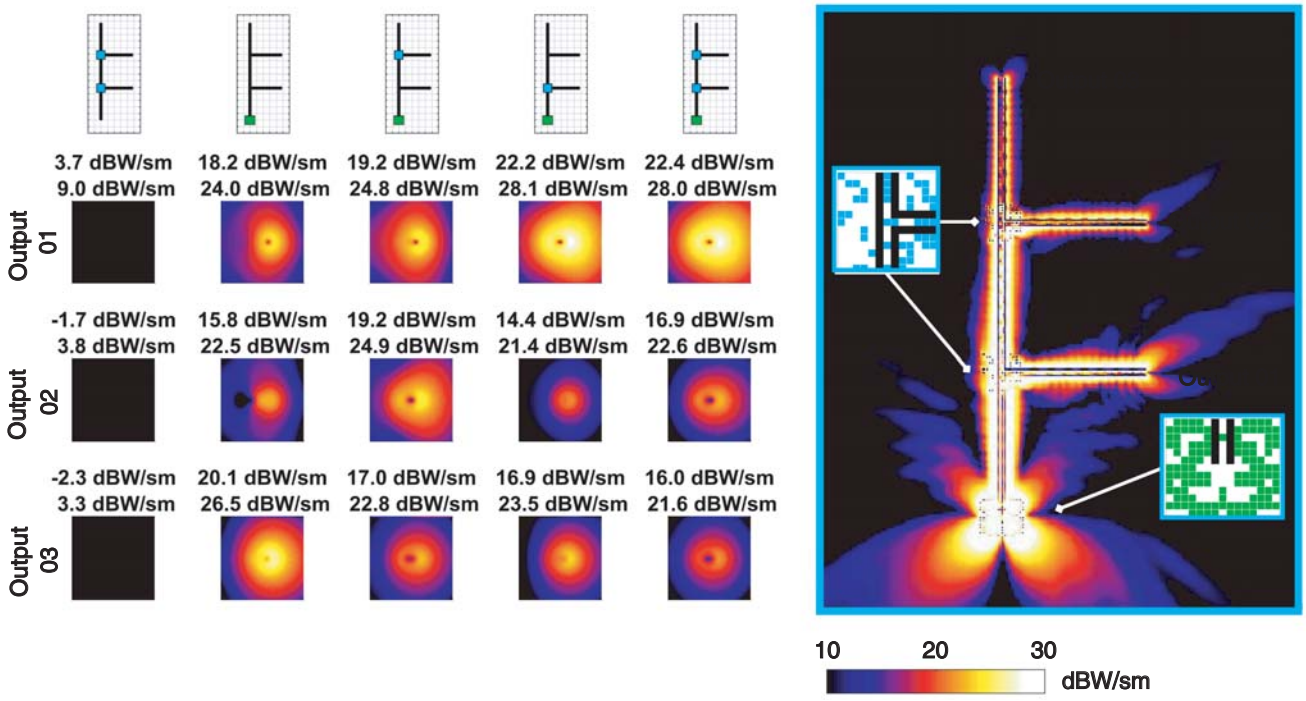

Figure 10. A nanowire system involving three outputs. In addition to the IC, two YCs are used for an efficient transmission of the power to the outputs.

In Fig. 11, we consider a system involving four symmetrically located outputs. Using only the IC at the input leads to 20.3 dBW/sm mean power density at Outputs 1 & 4 and 11.1 dBW/sm mean power density at Outputs 2 & 3. Further employing the FC and TC at the junctions improves the transmission to all outputs, leading to 21.1 dBW/sm, 15.9 dBW/sm, 15.7 dBW/sm, and 20.8 dBW/sm mean power density values at Outputs 1–4, respectively. We note that the FC balances the distribution of the power towards Output 1, Output 4, and the nanowire segment connected to the T-junction. Then, the TC divides the incoming power (from the FC) into two, towards Output 2 and Output 3.

Finally, Fig. 12 depicts a system involving nine nanowire segments (each with 5 μm length)

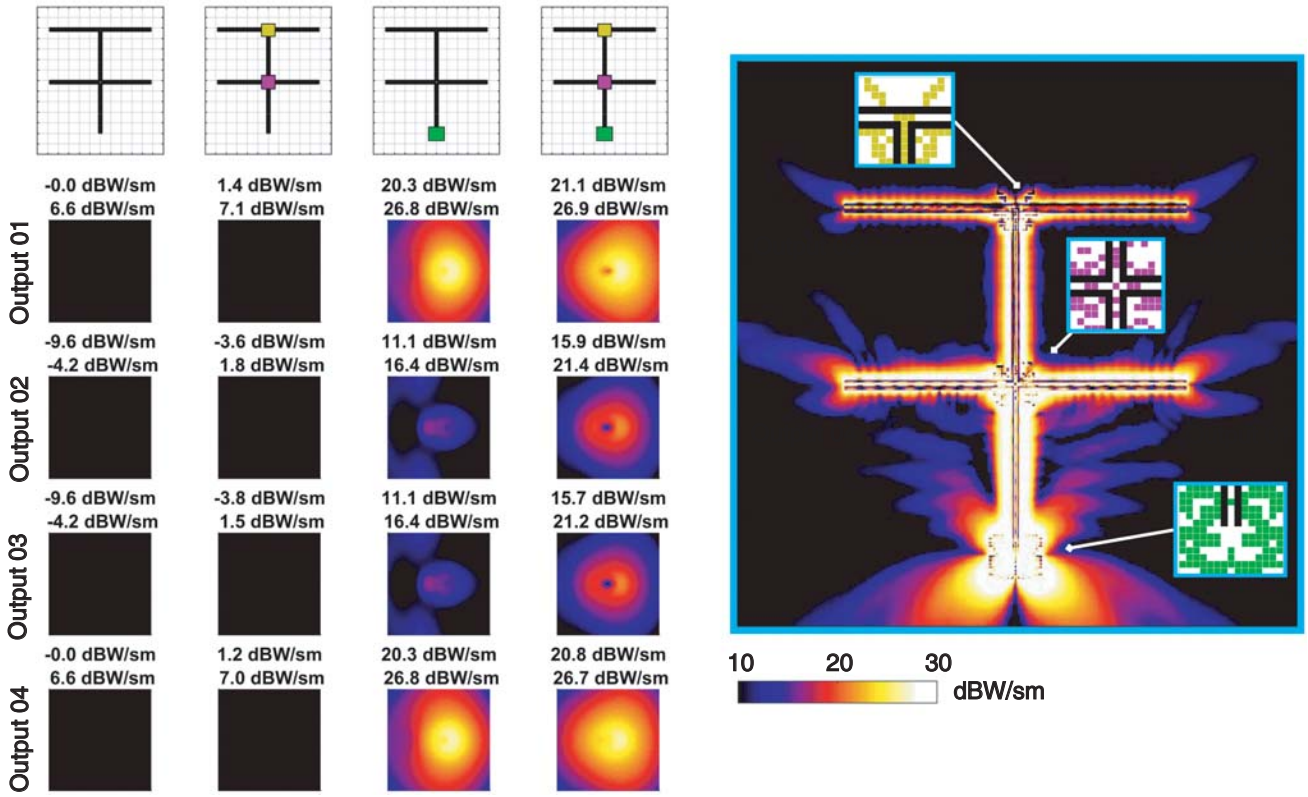

Figure 11. A nanowire system involving four outputs. In addition to the IC, the junctions are supported by the FC and TC to obtain an efficient transmission of the power to the outputs.

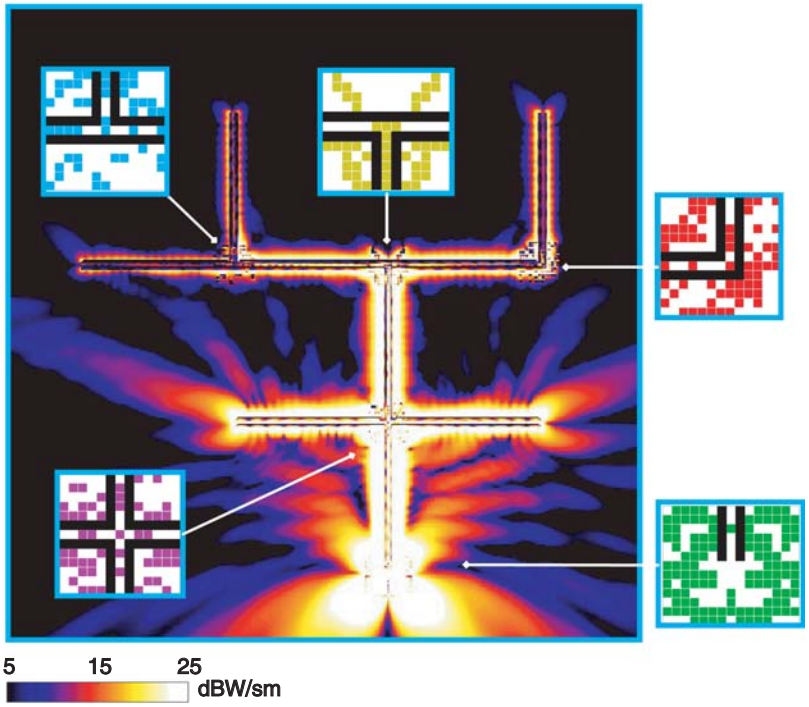

Figure 12. A nanowire system involving nine nanowire segments and five outputs. The power density distribution is shown for the full system with five different couplers used at suitable positions.

connected via all five couplers presented in this paper. The power density distribution for the entire geometry is depicted to illustrate the efficiency of the power transmission along the nanowires. Once the input power reaches the four-way junction, it is divided equally (by the FC) into three; towards two outputs (Outputs 1 and 5) and the vertical segment that is connected to the T-junction. At the T-junction, the TC further divides the incoming power into two. On the right-hand side, the power is transmitted to Output 2 after a sharp corner that is supported by the CC. On the left-hand side, the power is finally divided between a horizontal and a vertical segments via the YC to be transmitted to Outputs 3 and 4. The mean power density values are obtained as 21.1 dBW/sm, 10.8 dBW/sm, 7.7 dBW/sm, 8.2 dBW/sm, and 20.9 dBW/sm at Outputs 1–5, respectively, while these values are only 0.2 dBW/sm, −15.1 dBW/sm, −14.6 dBW/sm, −14.8 dBW/sm, and 0.2 dBW/sm without the couplers.

5. CONCLUSIONS

Design and analyses of efficient couplers consisting of well-designed arrangements of nanocubes to improve power transmissions in nanowire systems are presented. Given various grids of nanocubes, optimal arrangements are found by employing GAs and full-wave simulations of subsystems via MLFMA. The designed couplers are investigated in detail, both within their optimization setups and when they are combined. As they are designed in generic scenarios involving T-junction, Y-junction, and four-way junction, in addition to nanowire inputs and sharp corners, the couplers can be used in diverse combinations to build systems consisting of multiple nanowire segments and outputs. Various nanowire systems are presented to illustrate the harmony of the designed couplers to provide high-quality transmissions from inputs to outputs in challenging cases. The results also demonstrate the feasibility of constructing larger systems towards nano-optical networks based on nanowires and efficient couplers, while the interactions between the subsystems can again be analyzed via full-wave simulations.

ACKNOWLEDGMENT

This work was supported by the Scientific and Technical Research Council of Turkey (TUBITAK) under the Research Grant 118E243 and by the Turkish Academy of Sciences (TUBA) in the framework of the Young Scientist Award Program.

REFERENCES

1. Wang, X., C. J. Summers, and Z. L. Wang, "Large-scale hexagonal-patterned growth of aligned ZnO nanorods for nano-optoelectronics and nanosensor arrays," *Nano Lett.*, Vol. 4, No. 3, 423–426, Jan. 2004.
2. Ditlbacher, H., A. Hohenau, D. Wagner, U. Kreibig, M. Rogers, F. Hofer, F. R. Aussenegg, and J. R. Krenn, "Silver nanowires as surface plasmon resonators," *Phys. Rev. Lett.*, Vol. 95, No. 257403, Dec. 2005.
3. Sanders, A. W., D. A. Routenberg, B. J. Wiley, Y. Xia, E. R. Dufresne, and M. A. Reed, "Observation of plasmon propagation, redirection, and fan-out in silver nanowires," *Nano Lett.*, Vol. 6, No. 8, 1822–1826, Jun. 2006.
4. Akimov, A. V., A. Mukherjee, C. L. Yu, D. E. Chang, A. S. Zibrov, P. R. Hemmer, H. Park, and M. D. Lukin, "Generation of single optical plasmons in metallic nanowires coupled to quantum dots," *Nature*, Vol. 450, No. 7168, 402–406, Nov. 2007.
5. Yao, J., Z. Liu, Y. Liu, Y. Wang, C. Sun, G. Bartal, A. M. Stacy, and X. Zhang, "Optical negative refraction in bulk metamaterials of nanowires," *Science*, Vol. 321, No. 5891, 930, Aug. 2008.
6. Guo, X., M. Qiu, J. Bao, B. J. Wiley, Q. Yang, X. Zhang, Y. Ma, H. Yu, and L. Tong, "Direct coupling of plasmonic and photonic nanowires for hybrid nanophotonic components and circuits," *Nano Lett.*, Vol. 9, No. 12, 4515–4519, 2009.
7. Casse, B. D. F., W. T. Lu, Y. J. Huang, E. Gultepe, and L. Menon, "Super-resolution imaging using a three-dimensional metamaterials nanolens," *Appl. Phys. Lett.*, Vol. 96, No. 023114, Jan. 2010.

8. Wang, W., Q. Yang, F. Fan, H. Xu, and Z. L. Wang, "Light propagation in curved silver nanowire plasmonic waveguides," *Nano Lett.*, Vol. 11, No. 4, 1603–1608, Mar. 2011.
9. Bergin, S. M., Y. Chen, A. R. Rathmell, P. Charbonneau, Z. Y. Lib, and B. J. Wiley, "The effect of nanowire length and diameter on the properties of transparent, conducting nanowire films," *Nanoscale*, Vol. 4, No. 6, 1996–2004, Feb. 2012.
10. Huang, Y., Y. Fang, Z. Zhang, L. Zhu, and M. Sun, "Nanowire-supported plasmonic waveguide for remote excitation of surface-enhanced Raman scattering," *Light: Science and Applications*, Vol. 3, No. 199, Aug. 2014.
11. Yılmaz, A., B. Karaosmanoğlu, and Ö. Ergül, "Computational electromagnetic analysis of deformed nanowires using the multilevel fast multipole algorithm," *Sci. Rep.*, Vol. 5, No. 8469, Feb. 2015.
12. Şatana, H. A., B. Karaosmanoğlu, and Ö. Ergül, "A comparative study of nanowire arrays for maximum power transmission," *Nanowires*, K. Maaz, Ed., InTech, 2017.
13. Altınoklu, A. and Ö. Ergül, "Nano-optical couplers for efficient power transmission along sharply bended nanowires," *ACES J.*, Vol. 34, No. 2, 228–233, Feb. 2019.
14. Chew, W. C., J.-M. Jin, E. Michielssen, and J. Song, *Fast and Efficient Algorithms in Computational Electromagnetics*, Artech House, Boston, 2001.
15. Ergül, Ö. and L. Gürel, *The Multilevel Fast Multipole Algorithm (MLFMA) for Solving Large-Scale Computational Electromagnetics Problems*, Wiley-IEEE, 2014.
16. Karaosmanoğlu, B., A. Yılmaz, U. M. Gür, and Ö. Ergül, "Solutions of plasmonic structures using the multilevel fast multipole algorithm," *Int. J. RF Microwave Comput.-Aided. Eng.*, Vol. 26, No. 4, 335–341, May 2016.
17. Önol, C., B. Karaosmanoğlu, and Ö. Ergül, "Efficient and accurate electromagnetic optimizations based on approximate forms of the multilevel fast multipole algorithm," *IEEE Antennas Wireless Propag. Lett.*, Vol. 15, 1113–1115, Apr. 2016.
18. Altinoklu, A. and Ö. Ergül, "Computational design and analysis of efficient couplers for nano-optical links," *2019 PhotonIcs & Electromagnetics Research Symposium — Spring (PIERS-Spring)*, 91–99, Rome, Italy, Jun. 17–20, 2019.
19. Altınoklu, A., G. Karaova, and Ö. Ergül, "Design and analysis of nano-optical networks consisting of nanowires and optimized couplers," *Proc. Int. Conf. on Electromagnetics in Advanced Applications (ICEAA)*, 931–936, 2019.
20. Karaosmanoğlu, B., A. Yılmaz, and Ö. Ergül, "A comparative study of surface integral equations for accurate and efficient analysis of plasmonic structures," *IEEE Trans. Antennas Propag.*, Vol. 65, No. 6, 3049–3057, Jun. 2017.
21. Önol, C., A. Üçüncü, and Ö. Ergül, "Efficient multilayer iterative solutions of electromagnetic problems using approximate forms of the multilevel fast multipole algorithm," *IEEE Antennas Wireless Propag. Lett.*, Vol. 16, 3253–3256, 2017.
22. Rao, S. M., D. R. Wilton, and A. W. Glisson, "Electromagnetic scattering by surfaces of arbitrary shape," *IEEE Trans. Antennas Propag.*, Vol. 30, No. 3, 409–418, Mar. 1982.